NASA-CR-200085

NCC 2-833

FINAL PROGRESS REPORT,
December 1995

NASA GRANT NUMBER NCC 2-833

Controls Design with Crossfeeds for Hovering Rotorcraft Using Quantitative Feedback Theory

by

Principal Investigator:
Daniel J. Biezad

Graduate Assistant:
Rendy Cheng

NASA Ames Research Center
Aircraft Guidance and Navigation Branch
Moffett Field, CA 94035-1000

January 8, 1996

Rotorcraft Flight Control Design Using Quantitative Feedback Theory and Dynamic Crossfeeds

Rendy P. Cheng
Aeronautical Engineering Department
California Polytechnic State University, San Luis Obispo, CA.

Mark B. Tischler
U.S. Army Aviation and Troop Command
Ames Research Center, Moffett Field, CA.

Daniel J. Biezad
Aeronautical Engineering Department
California Polytechnic State University, San Luis Obispo, CA.

ABSTRACT

A multi-input, multi-output controls design with dynamic crossfeed pre-compensation is presented for a rotorcraft in near-hovering flight using Quantitative Feedback Theory (QFT). The resulting closed-loop control system bandwidth allows the rotorcraft to be considered for use as an inflight simulator. The use of dynamic, robust crossfeeds prior to the QFT design reduces the magnitude of required feedback gain and results in performance that meets most handling qualities specifications relative to the decoupling of off-axis responses. Handling qualities are Level 1 for both low-gain tasks and high-gain tasks in the roll, pitch, and yaw axes except for the 10 deg/sec moderate-amplitude yaw command where the rotorcraft exhibits Level 2 handling qualities in the yaw axis caused by phase lag.

The combined effect of the QFT feedback design following the implementation of low-order, dynamic crossfeed compensators successfully decouples ten of twelve off-axis channels. For the other two channels it was not possible to find a single, low-order crossfeed that was effective. This is an area to be investigated in future research.

1. NOMENCLATURE

G_{in}^{out}	Crossfeed relating "out" to "in" input controllers.
GROUP	Configuration sets (Group I most probable, Group III least probable)
CHANNEL	Degree-of-freedom in a control system.
MSW	Mean-Square Weighted
NAVFIT	Computer Program used to compute low-order "fits" to transfer functions.
IDEAL	Refers to "ideal constrained" analytical solution for crossfeed transfer functions.
TEMPLATE	Gain and phase value for "ideal constrained" crossfeeds at a specific ω.
TARGET	Refers to a heuristic decoupling crossfeed solution for a class of configurations.
ACHIEVED	Refers to a low-order transfer function "fit" to a set of "target" templates.
(a)	Short form for (s+a)
(ζ,ω)	Short form for $(s^2 + 2\zeta\omega s + \omega^2)$

2. INTRODUCTION

2.1 Background

NASA and the U.S. Army Aeroflightdynamics Directorate (AFDD) are developing a UH-60 Black Hawk helicopter to be used as the Rotorcraft Aircrew Systems and Controls Airborne Laboratory (RASCAL), an inflight simulator to evaluate fly-by-wire controls and systems concepts. A key goal of the flight control design for RASCAL is to achieve high bandwidth and decoupled response characteristics as required by the current helicopter handling-qualities specification ADS-33C (refs. 1-2).

One of the proposed control concepts being evaluated is a robust hovering control designed using Quantitative Feedback Theory (QFT) (ref. 3). This theory is appropriate because of the significant uncertainty in the modeled rotorcraft that is caused by the large variation in rotorcraft dynamics with all vehicle states included, making gain scheduling impractical. The QFT technique as applied here uses dynamic crossfeeds (i.e. transfer functions) to cancel off-axis outputs. It has been postulated that dynamic crossfeeds, by providing "feedforward" decoupling, reduce the magnitude of required feedback gains and thus enhance the effectiveness of a QFT design. Prior research has developed preliminary metrics and weighting strategies for dynamic crossfeed design using a small number of linearized configurations with three inputs and three outputs (ref. 4). In this work the techniques developed in Reference 4 are extended to a four-input, four-output (4x4) decoupling problem for approximately 23 near-hover conditions.

2.2 Rotorcraft Models

The rotorcraft models representing a 4x4 multiple-input, multiple-output (MIMO) system were generated on FORECAST, a computer simulation of the UH-60 originating at Sikorsky Aircraft and later modified at Ames Research Center and the University of Maryland (ref.5). The configurations were weighted based on likelihood of

occurrence and were corrected with flight test data to obtain accurate off-axis responses. The frequency range of interest for piloted angular-rate commands was 1.0 to 10.0 rad/sec and for heave commands was from 0.2 to 2.0 rad/sec.

2.3 Scope

The focus of this study is to reduce the off-axis coupled responses by designing robust, dynamic crossfeeds and to improve the on-axis response by designing QFT control laws so that desirable handling qualities are achieved in 23 near-hovering flight conditions. The full-order helicopter dynamics including engine model, rotor flapping modes, rotor lagging modes, dynamic inflow model, tail downwash, and tail sidewash are modeled to represent the cross-coupling more accurately. Cross-coupling characteristics are expected to vary greatly with flight conditions. The main focus of this research is to achieve acceptable decoupling characteristics for the most probable flight speed variations in

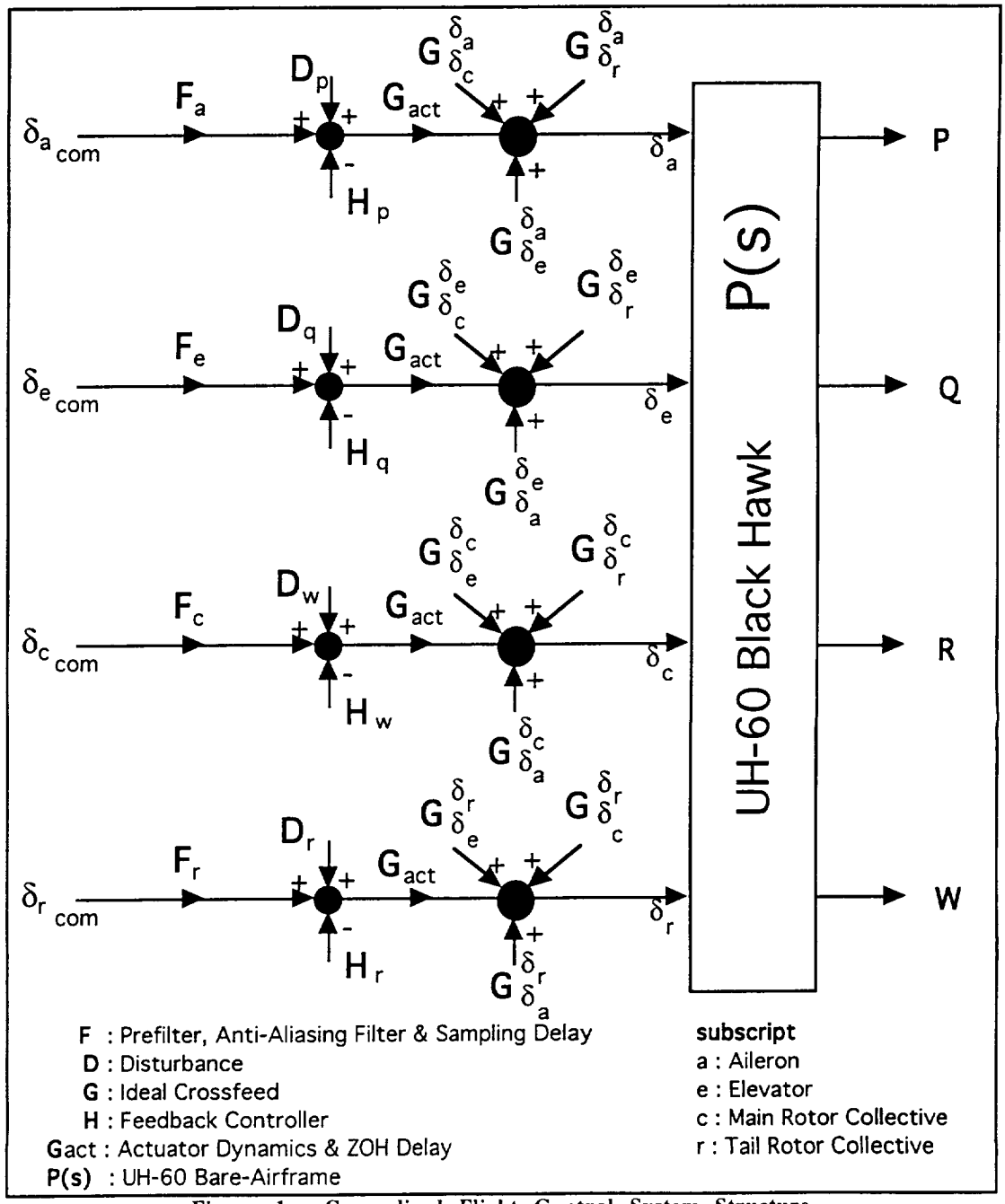

Figure 1. Generalized Flight Control System Structure

direction and speed up to 15 knots about a nominal hovering point of zero knots. Following this decoupling task, the resulting crossfeeds are included in the UH-60 dynamic model as a pre-compensator for a QFT feedback control law design. These additional feedbacks shape the on-axis responses to meet tracking performance and handling qualities criteria

2.4 Organization

In the next section coupling numerator theory (ref. 6-8) is applied to solve the generic 4x4 MIMO control problem using the concept of "constrained variables" developed in Reference 2. Following this the mathematical models are presented for the rotorcraft and range of flight configurations. The dynamic crossfeed design is then applied to the models, followed by the QFT design of control laws to meet specifications. A performance comparison is made showing the effectiveness of feedbacks and crossfeeds. Finally, the paper is concluded with an analysis of handling qualities relative to military rotorcraft specifications.

3. SYSTEM MODELING

The generalized block diagram representation of the rotorcraft is shown in Figure 1. The actuators are unity for this investigation. As an example of how the crossfeeds are labeled in the figure, note the locations of $G_{\delta_a}^{\delta_e}$ (referred to as "pitch (elevator)-from-aileron crossfeed") and $G_{\delta_e}^{\delta_a}$ (referred as "roll (aileron)-from-elevator crossfeed"). The first design task is to determine realizable, robust crossfeeds which reduce the magnitude of the feedback gains required to meet performance and handling qualities specifications.

3.1 Ideal Crossfeed Determination Using Coupling Numerators

The crossfeed and plant matrices of transfer functions in Figure 1 may be multiplied together to create an augmented open-loop system. "Ideal open-loop" decoupling crossfeeds can be determined analytically so that the resulting augmented open-loop system has a diagonal matrix relating outputs to inputs. However, even presuming that the analytical crossfeeds were physically realizable and stable, the sensitivity of the calculated analytical crossfeeds to plant parameter variations would be high.

To simplify the calculation of analytical "ideal" crossfeeds, the concept of "constrained variables" (ref. 9) is used to allow the crossfeed design to take into account the approximate effects of the feedback loops not yet synthesized at this stage of the control system formulation. Crossfeeds determined in this manner are called "ideal constrained" crossfeeds in that they mathematically decouple a system in the presence of a loop closure. The detailed technique and solution for "ideal constrained" crossfeeds is presented in Reference 10. The "ideal constrained" crossfeeds and the loop closures presumed for their determination are listed below in Tables 1-4.

Table 1. Responses to Lateral Cyclic, δa, Input

Control Coupling	Off-Axis	On-Axis
Pitch / Roll (Yaw constrained)	$\left[\frac{q}{\delta_a}\right]^{r}_{\delta_r} = \frac{N^{q\ r}_{\delta_a\delta_r} + G^{\delta_e}_{\delta_a} N^{q\ r}_{\delta_e\delta_r} + G^{\delta_c}_{\delta_a} N^{q\ r}_{\delta_c\delta_r}}{N^{r}_{\delta_r}}$	$\left[\frac{p}{\delta_a}\right]^{r}_{\delta_r} = \frac{N^{p\ r}_{\delta_a\delta_r}}{N^{r}_{\delta_r}}$
Yaw / Roll (Pitch constrained)	$\left[\frac{r}{\delta_a}\right]^{q}_{\delta_e} = \frac{N^{r\ q}_{\delta_a\delta_e} + G^{\delta_e}_{\delta_a} N^{r\ q}_{\delta_e\delta_e} + G^{\delta_c}_{\delta_a} N^{r\ q}_{\delta_c\delta_e}}{N^{q}_{\delta_e}}$	$\left[\frac{p}{\delta_a}\right]^{q}_{\delta_e} = \frac{N^{p\ q}_{\delta_a\delta_e}}{N^{q}_{\delta_e}}$
Heave / Roll (Pitch & Yaw constrained)	$\left[\frac{w}{\delta_a}\right]^{q\ r}_{\delta_e\delta_r} = \frac{N^{w\ q\ r}_{\delta_a\delta_e\delta_r} + G^{\delta_c}_{\delta_a} N^{w\ q\ r}_{\delta_c\delta_e\delta_r}}{N^{q\ r}_{\delta_e\delta_r}}$	$\left[\frac{p}{\delta_a}\right]^{q\ r}_{\delta_e\delta_r} = \frac{N^{p\ q\ r}_{\delta_a\delta_e\delta_r}}{N^{q\ r}_{\delta_e\delta_r}}$

Table 2. Responses to Longitudinal Cyclic, δe

Control Coupling	Off-Axis	On-Axis
Roll / Pitch (Yaw constrained)	$\left[\frac{p}{\delta_e}\right]_{\delta_r} = \frac{N^{p\,r}_{\delta_e\delta_r} + G^{\delta_a}_{\delta_e} N^{p\,r}_{\delta_a\delta_r} + G^{\delta_c}_{\delta_e} N^{p\,r}_{\delta_c\delta_r}}{N^{r}_{\delta_r}}$	$\left[\frac{q}{\delta_e}\right]_{\delta_r} = \frac{N^{q\,r}_{\delta_e\delta_r}}{N^{r}_{\delta_r}}$
Yaw / Pitch (Roll constrained)	$\left[\frac{r}{\delta_e}\right]_{\delta_a} = \frac{N^{r\,p}_{\delta_e\delta_a} + G^{\delta_a}_{\delta_e} N^{r\,p}_{\delta_a\delta_a} + G^{\delta_c}_{\delta_e} N^{r\,p}_{\delta_c\delta_a}}{N^{p}_{\delta_a}}$	$\left[\frac{q}{\delta_e}\right]_{\delta_a} = \frac{N^{q\,p}_{\delta_e\delta_a}}{N^{p}_{\delta_a}}$
Heave / Pitch (Roll & Yaw constrained)	$\left[\frac{q}{\delta_e}\right]_{\delta_a\delta_r} = \frac{N^{q\,p\,r}_{\delta_e\delta_a\delta_r}}{N^{p\,r}_{\delta_a\delta_r}}$	$\left[\frac{q}{\delta_e}\right]_{\delta_a\delta_r} = \frac{N^{q\,p\,r}_{\delta_e\delta_a\delta_r}}{N^{p\,r}_{\delta_a\delta_r}}$

Table 3. Responses to Tail Rotor Collective, δr, Input

Control Coupling	Off-Axis	On-Axis
Pitch / Yaw (Roll constrained)	$\left[\frac{q}{\delta_r}\right]_{\delta_a} = \frac{N^{q\,p}_{\delta_r\delta_a} + G^{\delta_e}_{\delta_r} N^{q\,p}_{\delta_e\delta_a} + G^{\delta_c}_{\delta_r} N^{q\,p}_{\delta_c\delta_a}}{N^{p}_{\delta_a}}$	$\left[\frac{r}{\delta_r}\right]_{\delta_a} = \frac{N^{r\,a}_{\delta_r\delta_a}}{N^{p}_{\delta_a}}$
Roll / Yaw (Pitch constrained)	$\left[\frac{p}{\delta_r}\right]_{\delta_e} = \frac{N^{p\,q}_{\delta_r\delta_e} + G^{\delta_a}_{\delta_r} N^{p\,q}_{\delta_a\delta_e} + G^{\delta_c}_{\delta_r} N^{p\,q}_{\delta_c\delta_e}}{N^{q}_{\delta_e}}$	$\left[\frac{r}{\delta_r}\right]_{\delta_e} = \frac{N^{r\,q}_{\delta_r\delta_e}}{N^{q}_{\delta_e}}$
Heave / Yaw (Roll & Pitch constrained)	$\left[\frac{w}{\delta_r}\right]_{\delta_a\delta_e} = \frac{N^{w\,p\,q}_{\delta_r\delta_a\delta_e} + G^{\delta_c}_{\delta_r} N^{w\,p\,q}_{\delta_c\delta_a\delta_e}}{N^{p\,q}_{\delta_a\delta_e}}$	$\left[\frac{r}{\delta_r}\right]_{\delta_a\delta_e} = \frac{N^{r\,p\,q}_{\delta_r\delta_a\delta_e}}{N^{p\,q}_{\delta_a\delta_e}}$

Table 4. Responses to Main Rotor Collective, δc, Input

Control Coupling	Off-Axis	On-Axis
Pitch / Heave (Roll & Yaw constrained)	$\left[\frac{q}{\delta_c}\right]_{\delta_a\delta_r} = \frac{N^{q\,p\,r}_{\delta_c\delta_a\delta_r} + G^{\delta_e}_{\delta_c} N^{q\,p\,r}_{\delta_e\delta_a\delta_r}}{N^{p\,r}_{\delta_a\delta_r}}$	$\left[\frac{w}{\delta_c}\right]_{\delta_a\delta_r} = \frac{N^{w\,p\,r}_{\delta_c\delta_a\delta_r}}{N^{p\,r}_{\delta_a\delta_r}}$
Roll / Heave (Pitch & Yaw constrained)	$\left[\frac{p}{\delta_c}\right]_{\delta_e\delta_r} = \frac{N^{p\,q\,r}_{\delta_c\delta_e\delta_r} + G^{\delta_a}_{\delta_c} N^{p\,q\,r}_{\delta_a\delta_e\delta_r}}{N^{q\,r}_{\delta_e\delta_r}}$	$\left[\frac{w}{\delta_c}\right]_{\delta_e\delta_r} = \frac{N^{w\,q\,r}_{\delta_c\delta_e\delta_r}}{N^{q\,r}_{\delta_e\delta_r}}$
Yaw / Heave (Roll & Pitch constrained)	$\left[\frac{r}{\delta_c}\right]_{\delta_a\delta_e} = \frac{N^{r\,p\,q}_{\delta_c\delta_a\delta_e} + G^{\delta_r}_{\delta_c} N^{r\,p\,q}_{\delta_r\delta_a\delta_e}}{N^{p\,q}_{\delta_a\delta_e}}$	$\left[\frac{w}{\delta_c}\right]_{\delta_a\delta_e\delta_r} = \frac{N^{w\,p\,q\,r}_{\delta_c\delta_a\delta_e\delta_r}}{N^{q\,p\,r}_{\delta_e\delta_a\delta_r}}$

3.2 Helicopter Mathematical Model: "FORECAST"

A linear mathematical model was generated for each of the UH-60 hovering configurations from the mathematical "truth" model described in Reference 11. Each linear model has 45 states: 6 states are attributable to the body motion, 16 states define the flap and lag motions of the rotor, 2 states describe the dynamic twist, 4 states represent the dynamic inflow, 6 states define the engine dynamics, 8 states describe the primary servo dynamics, 2 states define the downwash and

sidewash of the tail rotor, and one state defines the blade azimuth error.

The nominal flight condition is in hover at a gross weight of 16,825 lbs and the rotor speed set at 27 rad/sec. The 23 configurations result from variations in trim airspeed (longitudinal and lateral), rotor RPM, aircraft weight, center of gravity, turning rate, climb speed, and descending speed and were grouped subjectively by probability of occurrence. The groups were then assigned influence weightings used in the crossfeed design. The state space matrices (quadruples) of the linear model can be found in Appendix A of Reference 10.

3.3 Digital Control System Emulation

The control system structure is shown in Figure 2. A common method in digital flight control system design is to select the compensation based on an equivalent analog block diagram. Approximating analog effects are shown in Figure 2 for the digital-to analog converter (ZOH), signal sampler, anti-aliasing filter, and computational time delay (ref. 2).

The most important contributions to the time-delay for a digital system and their approximated transfer functions are shown in Table 5. The aircraft dynamics include the UH-60 dynamics and two sets of actuator dynamics which represent the fly-by-wire driver actuators and the UH-60 primary actuator. The total loop time delay of the system is 145 msec.

3.4 Determining Necessary Crossfeeds

Frequency sensitive metrics developed in Reference 4 were used to indicate whether or not decoupling a specified degree of freedom would be effective. By the reasoning of Reference 4, a metric value of 20 dB (factor of 10) or more for decoupling between a particular input and output channel shows that a crossfeed is not required between those channels because adequate decoupling already exists. Note by referring back to Figure 2 that it is possible to design 12 crossfeeds for the 4x4 system.

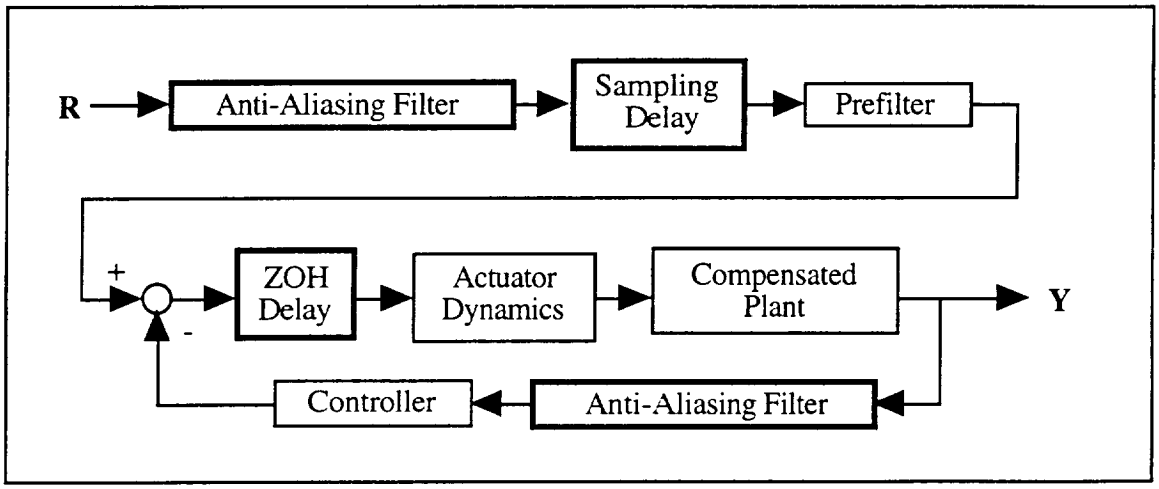

Figure 2 Digital Control System Structure

Table 5. Digital Control System Component Time-Delay

Time-Delay Types	Time-Delay, msec	Transfer Functions
Actuator Dynamics	36	$\frac{1521}{[0.7, 39]}$
Computation Delay & ZOH	15	$\frac{-(-133.33)}{(133.33)}$

Anti-Aliasing Filter	18	
Sampler Delay	10	$\frac{-(-200)}{(200)}$
Rotor Dynamics	66	*

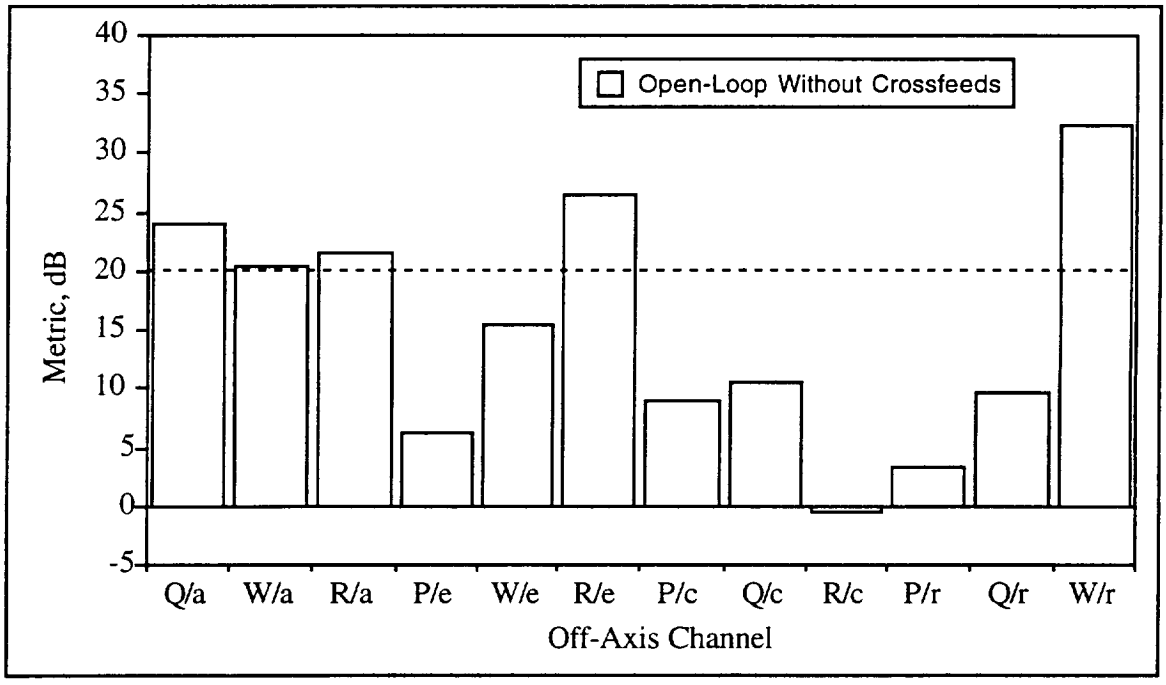

Figure 3. Decoupling Performance Metrics for the UH-60 (Open-Loop)

However, the decoupling metric values shown in Figure 3 indicate that only 7 crossfeeds are necessary (those columns below the 10 dB dotted line).

3.5 Approximating "Ideal Constrained" Crossfeeds

* Rotor dynamics time delays, including primary servos delays, are in the Forecast helicopter model.

In many cases the "ideal constrained" crossfeeds that mathematically decouple the outputs from the inputs are high-order transfer functions with unstable poles that are not practical to implement. Practical, stable, dynamic crossfeeds are obtained by approximating the "ideal constrained" crossfeeds with low-order (LO) equivalent transfer functions over the frequency range of interest. The LO crossfeed fit results were obtained from NAVFIT (ref. 12), and the typical NAVFIT approximating accuracy is shown for illustration purposes only in Figure 4.

In actuality the NAVFIT program fit a transfer function to "target" points based on frequency templates for the "ideal constrained" analytical crossfeeds. The data scatter in these templates determined the influence weighting of the template in the NAVFIT program. The hovering configurations were divided into three groups: Group I for most probable, Group II for less probable, and Group III for least probable.

Thus the LO dynamic crossfeed was not selected to approximate the "ideal constrained" analytical crossfeed of any particular one of the 23 configurations in hover. Instead, the LO dynamic crossfeed approximated the "target" crossfeed gain and phase values at specified frequencies as depicted in Figure 4. These gain and phase "target" values were chosen to represent the characteristics in a probabalistic sense for the 23 configurations using a process described in Reference 9. This process is based on the Mean Square Weighting (MSW) and coupling variance strategy also explained in Reference 9. The LO transfer function (constrained to be both stable and realizable) that best fits the "target" points is called the "achieved" transfer function fit. This "achieved" crossfeed is implemented in the control law design to follow. The seven "achieved" low-order dynamic crossfeeds for the rotorcraft are shown in Table 6 in shorthand form.

Note that all but one of the resulting crossfeeds were implemented using transfer functions instead of fixed-gains. These LO "achieved" dynamic crossfeeds were implemented using the MATLAB analysis package to obtain the decoupling metric value. The impact of the "achieved" crossfeeds on the open-loop system decoupling metrics can be seen in Figure 5. Note that only three of seven LO "achieved" crossfeeds result in significant improvement in decoupling performance (R/c, P/r, and Q/r). This is probably due to the large scatter in the "ideal constrained" crossfeed gain and phase values for the 23 configurations (not shown). Such scatter makes it difficult to obtain "target" gain and phase values in the piloted frequency range that are representative of the most probable of the 23 configurations. The Mean Square Weighting strategy thus may break down when parameter variation causes excessive scatter in the frequency domain. This is an area where future research is recommended.

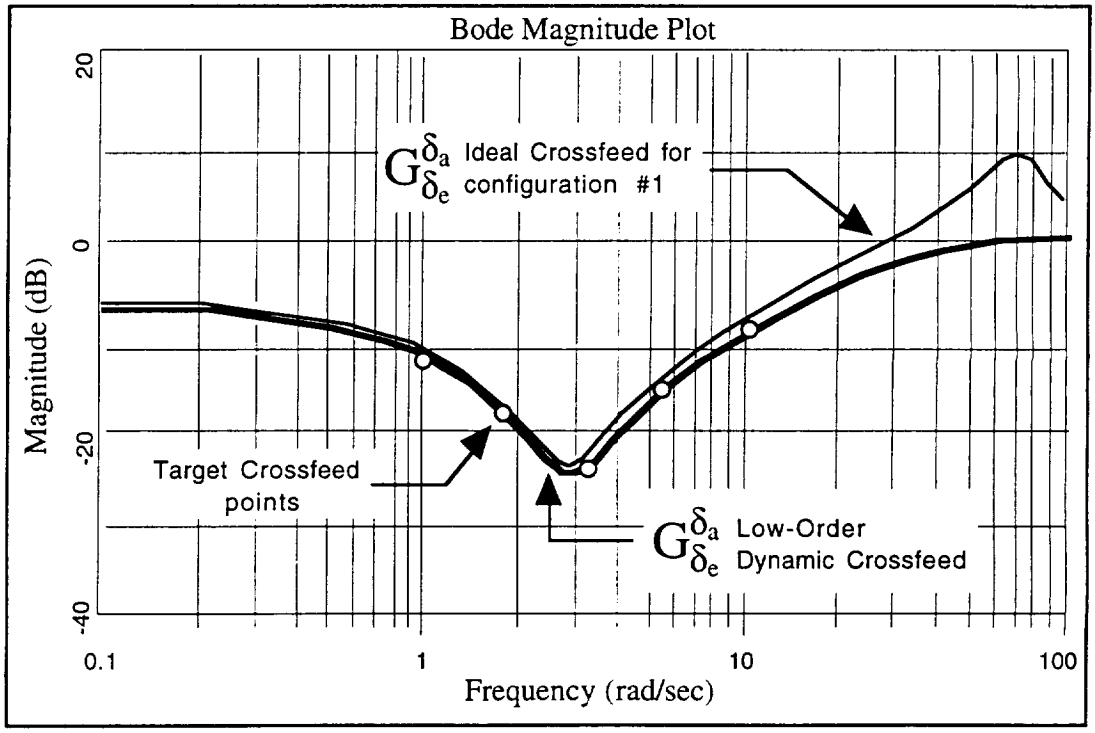

Figure 4. Low-Order (LO) Fit to Ideal Crossfeed

Table 6. "Achieved" Crossfeed Transfer Functions

$G_{\delta_e}^{\delta_a}$	$\frac{1.1829\,[0.3,\ 3.0]}{(0.6812)(30)}$
$G_{\delta_e}^{\delta_c}$	$\frac{6.5032}{(1.5712)(6.9965)}$
$G_{\delta_c}^{\delta_a}$	$\frac{0.01536\,[0.9487,\ 4.5915]}{[0.5475,\ 1.7705]}$
$G_{\delta_c}^{\delta_e}$	$\frac{0.1688\,[0.3519,\ 1.0825]}{(0.4834)(3.0)}$
$G_{\delta_c}^{\delta_r}$	$\frac{-0.1827\,(6.0)}{[0.3120,\ 2.3669]}$
$G_{\delta_r}^{\delta_a}$	0.3377
$G_{\delta_r}^{\delta_e}$	$\frac{4.2087}{(9.4877)}$

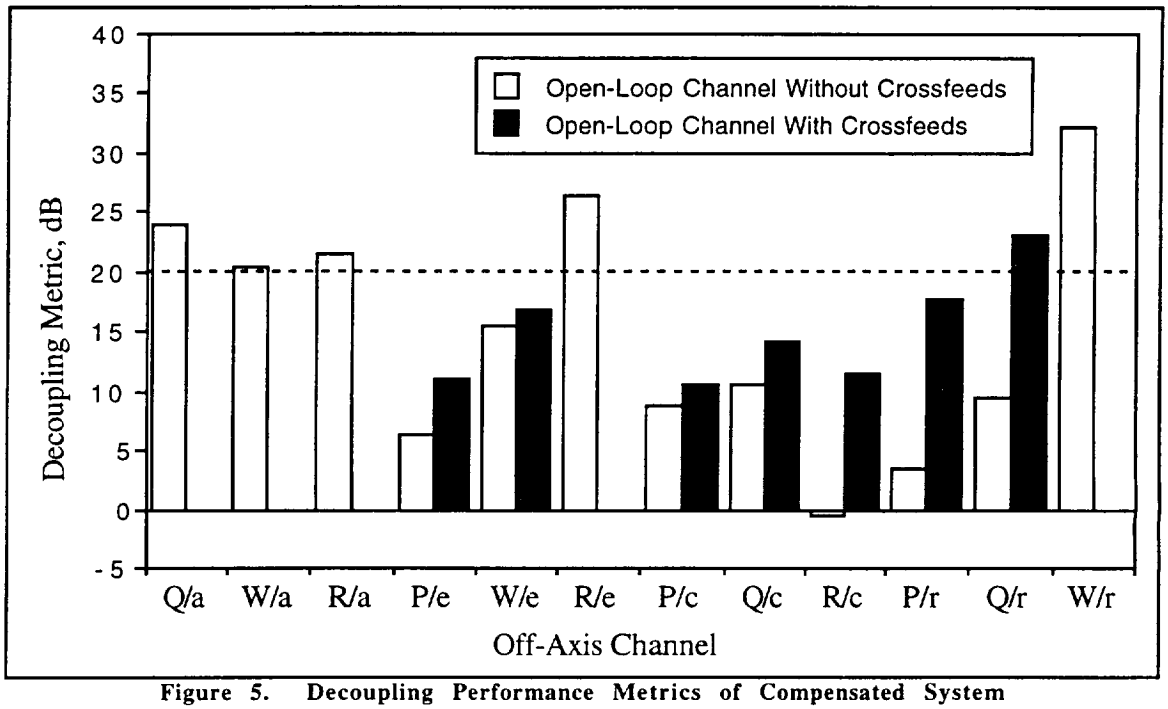

Figure 5. Decoupling Performance Metrics of Compensated System

4. QFT CONTROL DESIGN

Quantitative Feedback Theory may now be applied to the 23 configurations of the open-loop plant pre-compensated with the seven LO crossfeeds described in the previous section. Figure 6, taken from ADS-33C (Reference 13), is used to select a crossover frequency of 2.5 rad/sec for the roll, pitch, and yaw axes. The rectangular boxes (one for yaw and one for both roll and pitch) show the design boundaries selected for all 23 configurations. Designing to the specifications in the shaded boxes should provide Level 1 handling qualities (at least for small excitation piloted inputs).

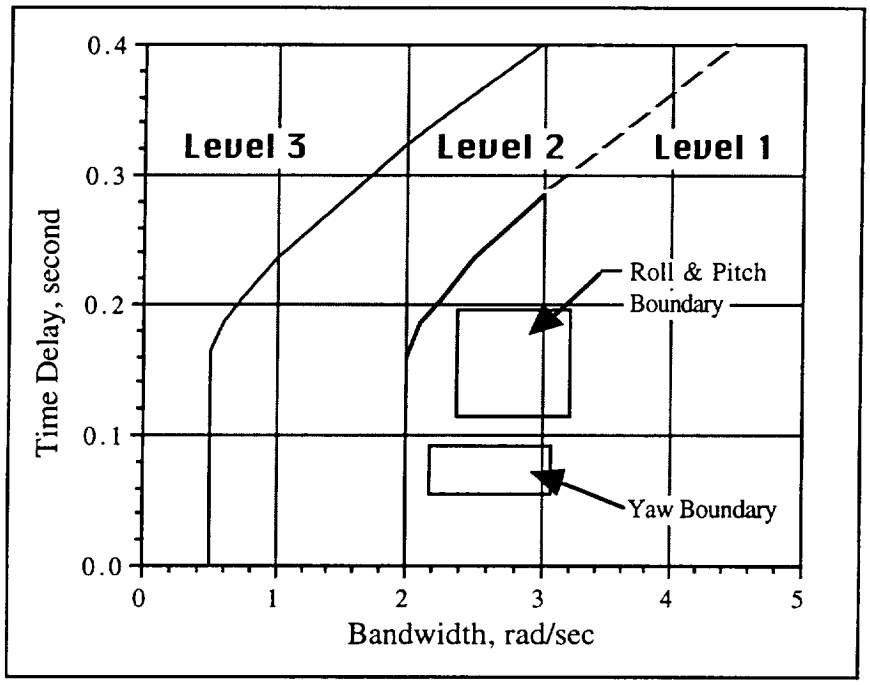

Figure 6 Design Point Criteria Selection

4.1 Tracking Performance: Specifications & Response Types

Tracking performance bounds are determined by using second and third order transfer functions to establish frequency bounds which have been selected to meet the handling qualities specification of Reference 13 (plus 10% overshoot) for a step input. The transfer functions are listed in Table 6.

For example, the frequency responses of all flight configurations for the roll and pitch axes must be between the bounds specified in the first row of Table 6 between 1 to 10 rad/sec. Falling outside of bounds at the lower frequencies near 1 rad/sec will not provide the desired steady state tracking performance; falling outside of bounds at higher frequencies near 10 rad/sec will not provide the desired transient response.

4.2 Controller Design

The low-order "achieved" crossfeeds designed are intended to decoupled the multi-input multi-output (MIMO) system into four single-input, single-output control system (SISO) as shown in Figure 7.

To simplify the controller only constant gains were chosen. Figure 8 shows the actual implementation of the QFT controller. The zero-order hold (ZOH) and anti-aliasing filter (AA) are added for digital control system emulation to simulate time delay and to reduce sensor noise.

The gains were designed to meet the tracking bounds of Table 6 and the standard QFT stability margin criteria (2.3 dB overshoot and 6 dB gain margin) using the QFT CAD package of Reference 14. The resulting controller gains are listed in Table 7.

Table 6. Tracking Performance Transfer Functions

Control Axis	Upper Bound	Lower Bound	Frequency Range
Roll, Pitch Axis	$\frac{8.3190\, e^{-0.143s}}{[0.45,\ 2.75]}$	$\frac{27.34\, e^{-0.143s}}{[0.75,\ 2.25](6.0)}$	1 - 10 rad/sec
Yaw Axis	$\frac{5.5\, e^{-0.077s}}{(0)(5.0)}$	$\frac{36\, e^{-0.050s}}{(0)(5.0)(8.0)}$	1 - 10 rad/sec
Heave Axis	$\frac{2.2e^{-0.077s}}{(0)(2.0)}$	$\frac{6.3e^{-0.050s}}{(0)(1.0)(7.0)}$	0.2 - 2.0 rad/sec

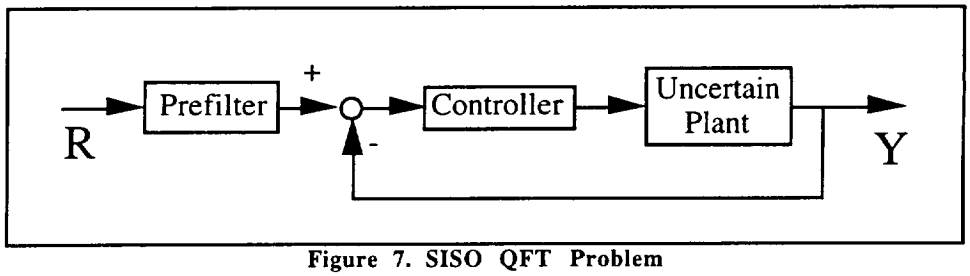

Figure 7. SISO QFT Problem

Table 7. QFT Controller Gains

	Rate Feedback Gain	Attitude Feedback Gain	Crossover Freq.(r/s)
Roll Axis	0.0222	0.1111	2.57
Pitch Axis	0.1089	0.0653	2.56
Heave Axis	0.1759	0.0633	1.05
Yaw Axis	0.1064	0.0255	2.42

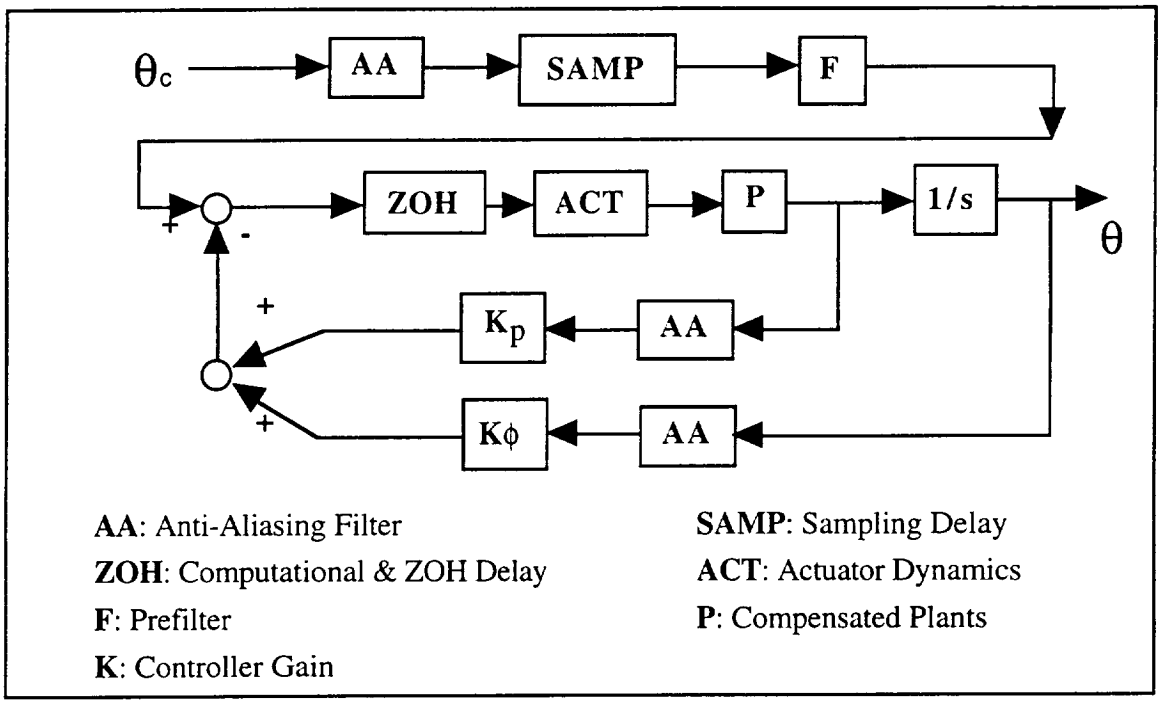

Figure 8. QFT Controller Implementation Structure

4.3 Prefilter Design

The purpose of the prefilter in QFT design is to ensure the resulting frequency response lies within tracking bounds which are determined by the transfer functions in Table 6. Because the handling qualities evaluations are determined mainly from the phase curve, final frequency responses must satisfy the tracking requirements in both magnitude and phase. Unfortunately, the QFT-CAD package in Reference 14 can only satisfy the magnitude bounds. The program NAVFIT of Reference 12, however, can be used to obtain the needed phase data as described below.

First, a series of midpoints for the desired closed-loop system with the prefilter called "GCL" are determined within the piloted frequency range between the tracking bounds for both the magnitude and phase curves. The frequency ranges for the piloted task are 0.3-20.0 for roll, pitch, and yaw axes, and 0.07-3.0 rad/sec for the heave axis. Now call the midpoints for the closed-loop response without the prefilter for nominal plant

"GP and determine their value. A set of frequency data

called "F" for the prefilter can be calculated by subtracting "GP" from "GCL ". By applying NAVFIT to approximate "F", the low-order prefilter transfer function can be find that satisfies the tracking bounds in both gain and phase values.

Finding a prefilter using the above procedure for the nominal plant does not guarantee that all remaining 22 configurations will also satisfy the tracking bounds in both gain and phase. If the plant variation is significantly narrower than the tracking boundary limits over the frequency range of interest a problem should not develop. On the other hand, when the tracking bounds are too tight, it is possible that a low-order prefilter cannot be found satisfying both gain and phase boundaries. A typical prefilter design plot is shown in Figure 9. This is also a recommended area for future research.

Because both the heave and yaw axes are rate command systems, an integrator is added to the prefilter designs which are shown in Table 8, and the entire design including crossfeed is depicted in Figure 10.

Table 8. QFT Prefilter

Control Axis	Transfer Function
Roll Axis	$\frac{2.4069\,[0.3098,\ 5.6726]\,(10)}{[0.5,3.7272]\,(44.075)}$
Pitch Axis	$\frac{10.7542\,(0.87279)(1.4151)}{[0.5571,\ 1.8887]\,(49.864)}$
Heave Axis	$\frac{0.18311\,(0.33296)}{(0)}$
Yaw Axis	$\frac{0.089825\,(0.15479)(8.0824)}{(0)(5.8870)}$

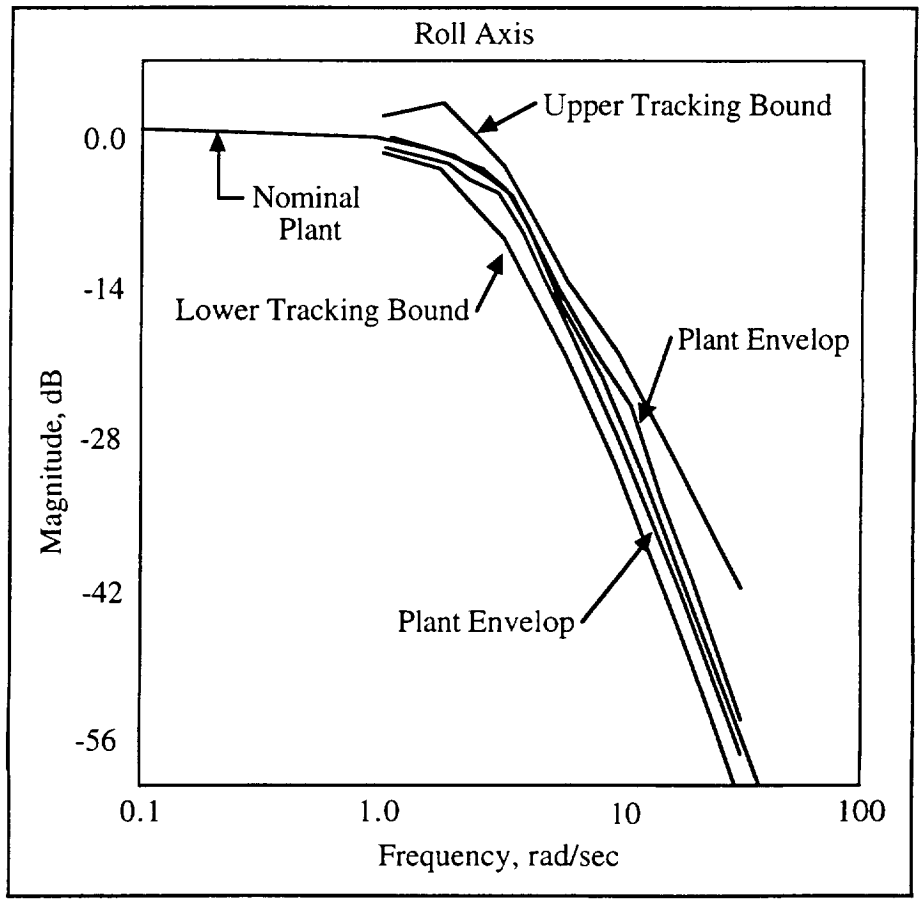

Figure 9. QFT Prefilter Design

5. ANALYSIS

5.1 Control Law Effects on Decoupling for the Closed-Loop System

The resulting performance of the closed-loop system is evaluated using the decoupling metrics previously described and shown in Figure 11. For those input-output pairs where crossfeeds were needed (gray columns), in all but two cases (P/e and W/e) the QFT control law achieved significant additional decoupling (see for example P/c, Q/c, and R/c in Figure 11).

5.2 Net Effect of Dynamic Crossfeeds on the Closed-Loop System

The resulting net effect of the "achieved" crossfeeds on the decoupling performance of the closed-loop system is shown in Figure 12. In this figure, the "achieved" crossfeeds improve the decoupling metric most for the yaw-from-collective (R/c), roll-from-rudder (P/r), and pitch-from-rudder (Q/r) channels. It is thus apparent that, at least for the R/c, P/r, and Q/r channels (white

columns on the right half of Figure 12), the closed-loop control law without crossfeeds would have to work harder (that is, be redesigned with larger gains) in order to match the performance of the closed-loop system with crossfeeds (gray columns in Figure 12).

5.3 Handling Qualities Analysis

The handling qualities analysis is based on the *Handling Qualities Requirements for Military Rotorcraft* (Reference 13). In this study, three types of requirement are tested: Small-, Moderate-, Large-Amplitude Attitude Changes. All three requirements are evaluated by two variables: bandwidth and phase delay. The handling qualities results of small-amplitude roll, pitch, or yaw attitude changes of all 23 flight configurations for hover and low speed are Level 1 and are shown in Figure 13. All the Group I and II closed-loop configurations have frequency responses within the boundary defined in Table 6. All the cases outside of the boundary belong to group III which has the least weighting value.

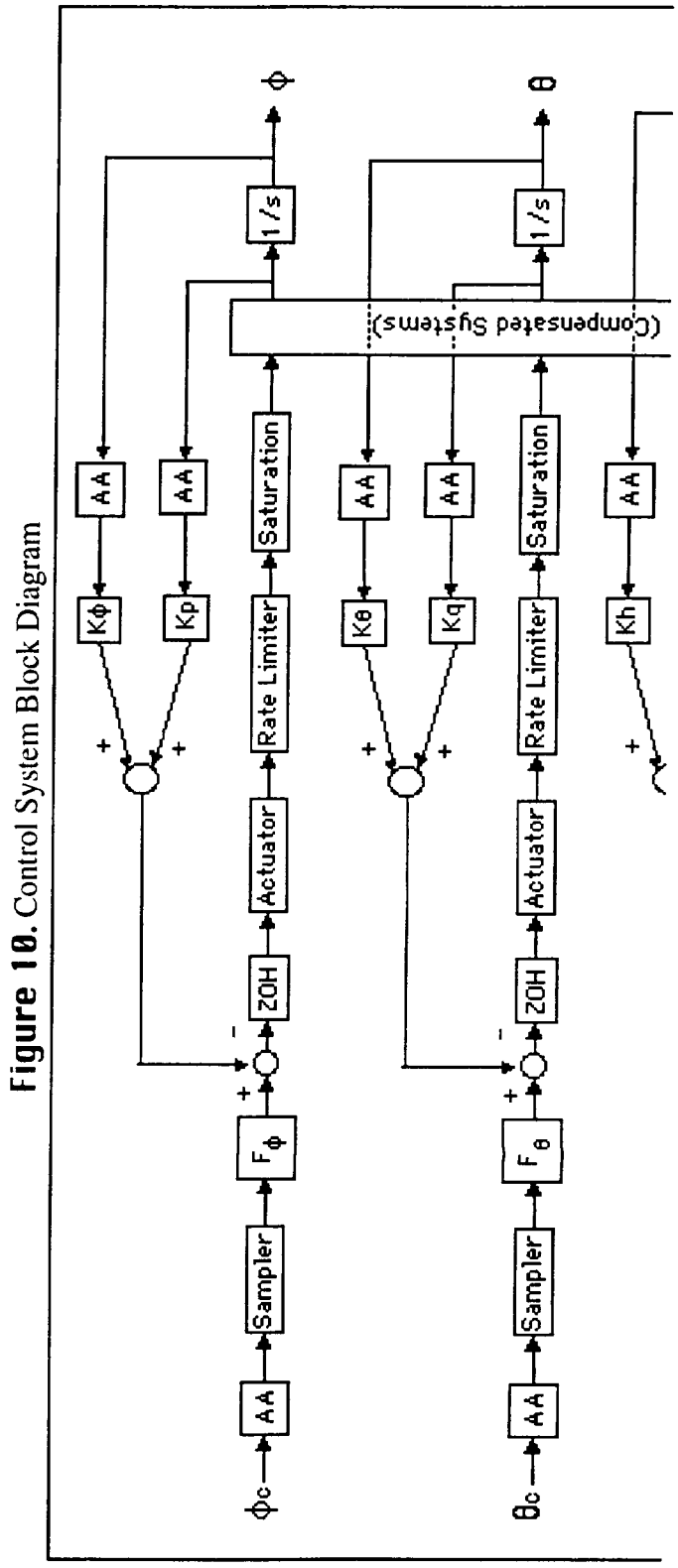

Figure 10. Control System Block Diagram

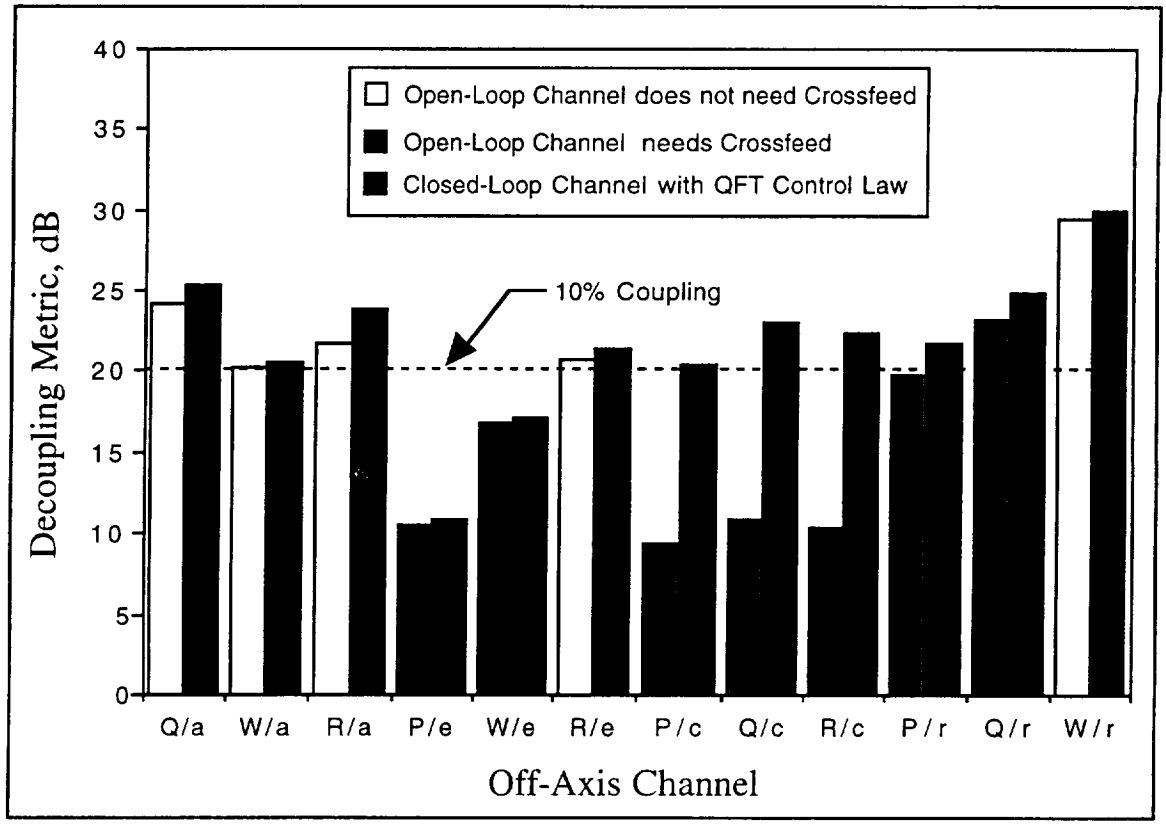

Figure 11. Decoupling Metric of Closed-Loop System

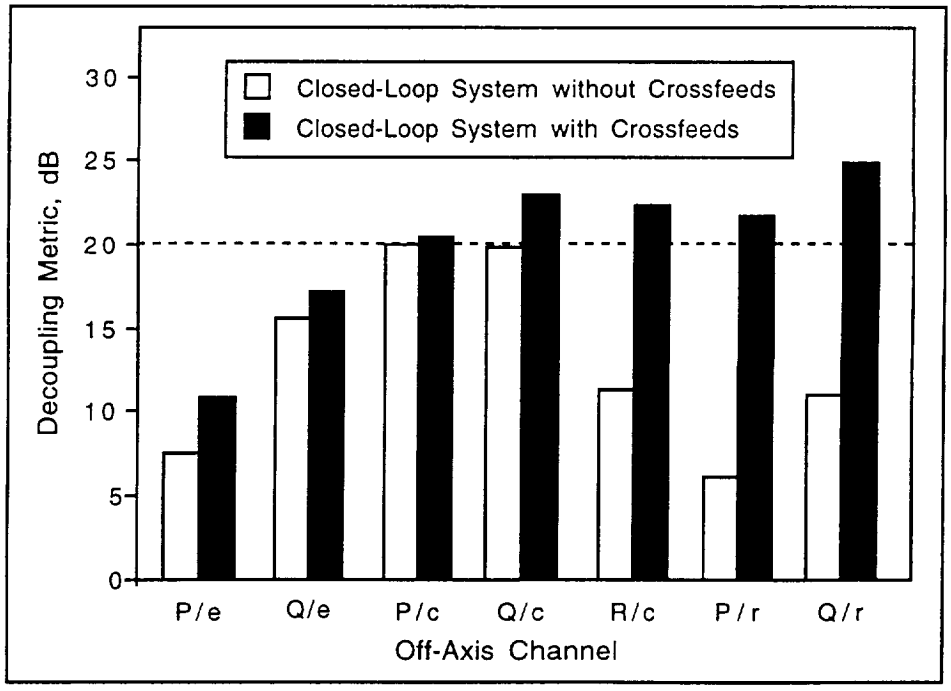

Figure 12 Effect of the Low-Order Dynamic Crossfeeds

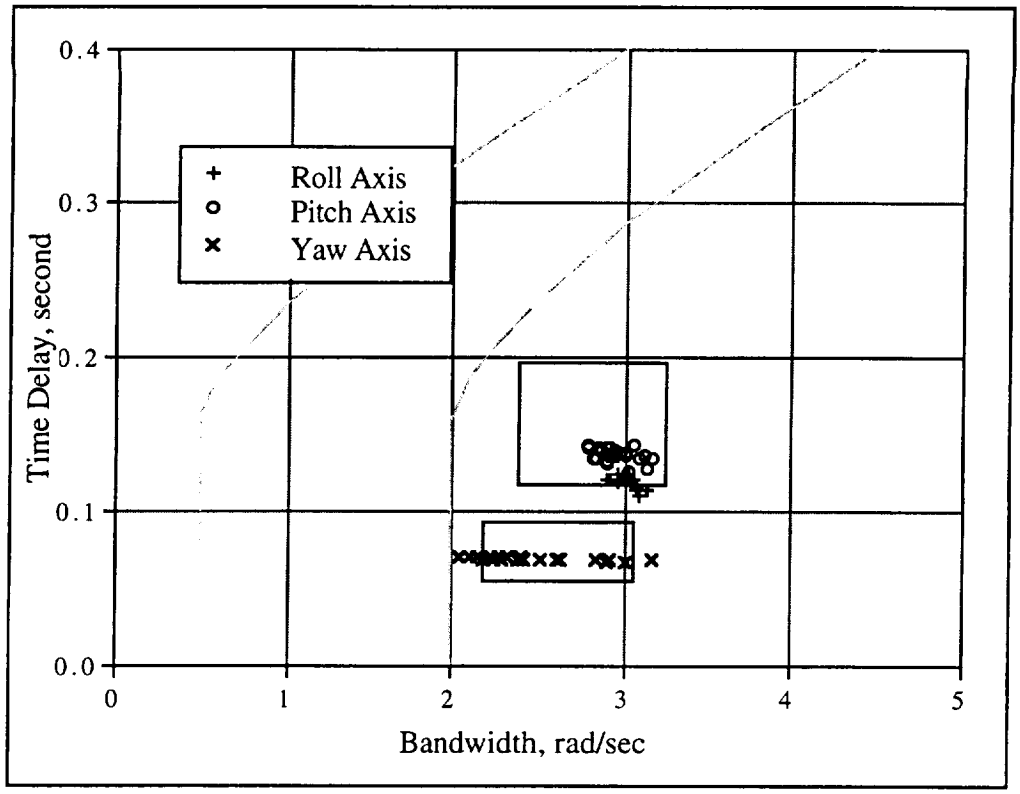

Figure 13. Requirements for Small-Amplitude Attitude Changes_

5.4 Moderate-Amplitude Attitude Change

In the moderate-amplitude attitude change requirement (quickness), the aircraft attitude is abruptly commanded to change at least 10° in either the roll or yaw axis, and at least 5° in the pitch axis. The required attitude changes should be made as rapidly as possible from one steady attitude to another without significant reversals in the sign of the cockpit control input relative to the trim position. The specification then evaluates the resulting peak rate achieved to the peak angle achieved. The handling qualities results of moderate-amplitude roll (pitch, yaw) attitude changes for hover and low speed flight are shown in Figure 14. The figures show that the handling
qualities for the roll and pitch axes are Level 1, but Level 2 for the yaw axis. The main cause of the Level 2 rating is insufficient yaw-axis control power.

5.5 Large-Amplitude Attitude Change

Under this requirement, the aircraft has to obtain a bank angle of ±60°, pitch angle of ±30°, and a yaw rate of ±60 deg/sec in a rapid hovering turn that evaluates aggressive maneuvering (see Section 3.3.4 of Reference 1). The aircraft was Level 1 in all three axes.

5.6 Collective-to-Yaw Coupling Requirement

The handling qualities specification for the vertical axis is a collective-to-yaw coupling requirement which evaluates vertical axis performance. As shown in Figure 15, the rotorcraft is Level 1 for this requirement. Axis labels are explained in Section 3.3.9.1 of Reference 1.

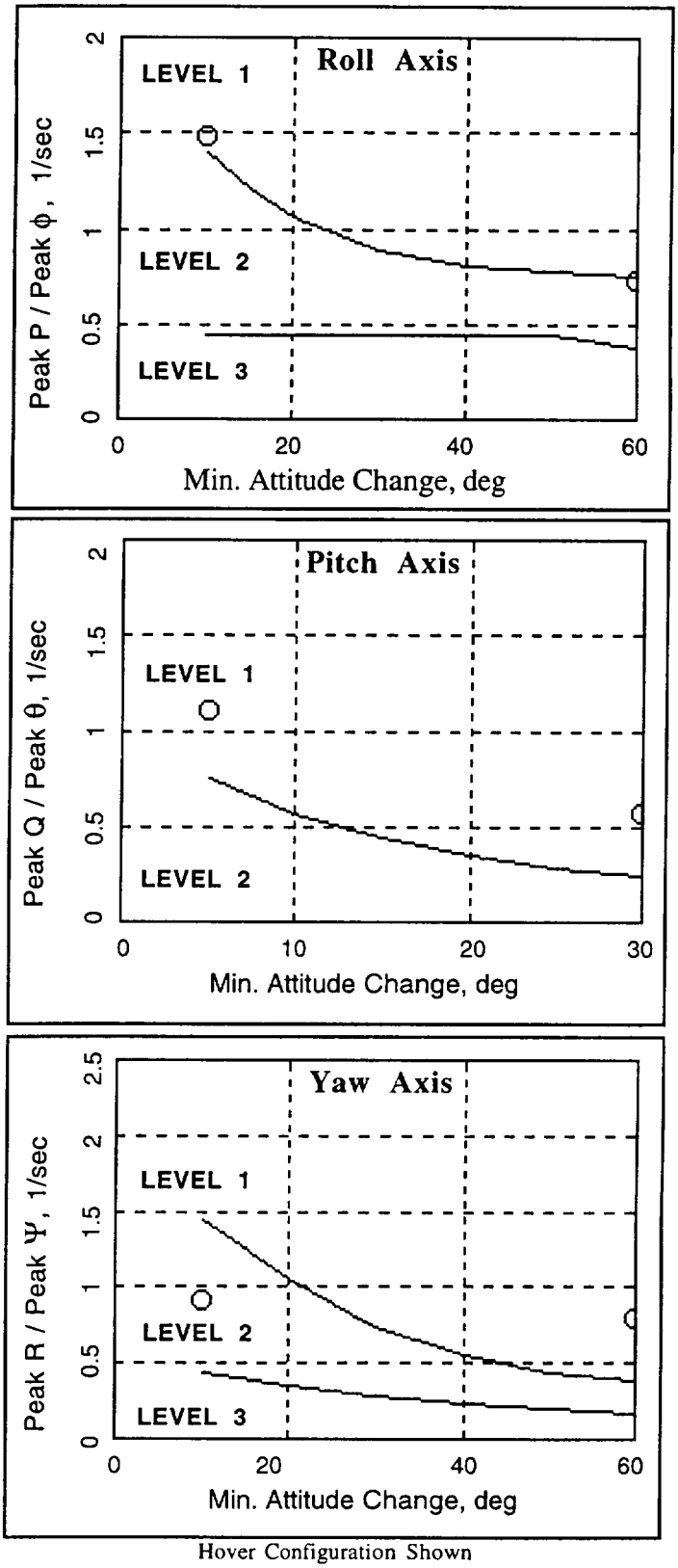

Hover Configuration Shown

Figure 14. Requirements for Moderate- & Large-Amplitude Attitude Changes